Demo: Now You See It! RIS-Assisted mmWave Radar for NLOS Sensing

Joana Angjo Anatolij Zubow Christos Laskos Falko Dressler
TU Berlin, EECS
Berlin, Germany
{angjo, zubow, laskos, dressler}@ccs-labs.org

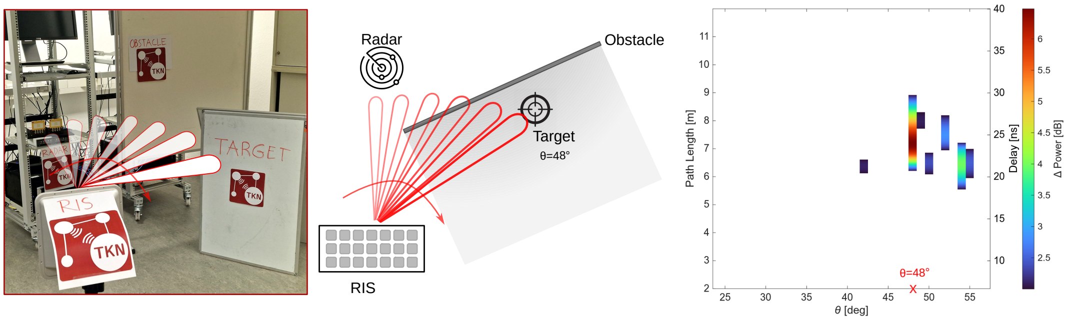

Figure 1: Testbed with the target, bird's-eye-view illustration, and the positive differential power delay profile (PDP) obtained by subtracting the PDP of the calibration experiment from that with the target present.

Abstract

Target detection via radar is a fundamental sensing capability, but at mmWave frequencies visibility in non-line-of-sight (NLOS) is sharply limited by obstacles and high attenuation. Reconfigurable intelligent surfaces (RIS) are widely proposed as a solution to this. However, many approaches either address moving targets, exploiting motion-induced changes in multipath, or are only evaluated in simulation. In this demo, we present a software-defined radio testbed, in which an RIS enables a monostatic radar to detect a static, passive target in NLOS. Detection is performed through a low-cost differential per-RIS-angle between a reference and target-present measurements. Attendees can process real measurements and observe how RIS beam steering exposes an otherwise undetectable target, illustrating the potential of programmable wireless environments for practical NLOS sensing.

Keywords

reconfigurable intelligent surface, non-line-of-sight sensing, monostatic radar, millimeter wave, software defined radio

MobiCom '26, Austin, TX, USA

ACM ISBN 978-1-4503-XXXX-X/2018/06
https://doi.org/10.1145/3795866.3848436

ACM Reference Format:
Joana Angjo Anatolij Zubow Christos Laskos Falko Dressler. 2026. Demo: Now You See It! RIS-Assisted mmWave Radar for NLOS Sensing. In *The 32nd Annual International Conference on Mobile Computing and Networking (MobiCom '26), October 26–30, 2026, Austin, TX, USA.* ACM, New York, NY, USA, 3 pages. https://doi.org/10.1145/3795866.3848436

1 Introduction

mmWave radar is attractive for high-resolution sensing because its large available bandwidth improves range resolution, while the dense antenna arrays improve angular resolution. Yet, conventional radars are typically designed to operate under line of sight (LoS), and detection of objects shadowed by obstacles is usually not feasible. Moreover due to less diffraction and higher attenuation, naturally occurring multipath is weak and unreliable. Reconfigurable intelligent surfaces (RIS) allow for programmable reflections, while providing enhanced angular resolution, thus they have proven advantageous in the literature for enabling non-line-of-sight (NLOS) radar [1].

MetaSight uses fully passive metasurfaces, keeping deployment complexity low, but fixes the angular mapping at fabrication: the covered NLOS sector is fixed by design and cannot be dynamically retargeted [5]. Horus deploys RIS-assisted roadside infrastructure to detect road users hidden from an approaching vehicle; however, the radar itself has an unobstructed path to the target [3]. PRISM varies the

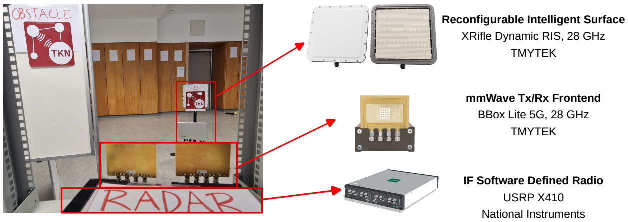

Figure 2: Testbed components (radar's perspective).

configuration of RIS elements at a rate of several MHz and the evaluation is done in post-processing [4]. RFlect exploits naturally available reflecting surfaces for NLOS imaging, making its solution dependent on the geometry of the available reflectors [2]; while RISE reconstructs an environment by resolving the multipath generated by a moving human [7]. Similarly, [6] also shows the benefits of RIS for around-the-corner human detection via micro-Doppler signatures.

To the best of our knowledge, a programmable hardware system combining a monostatic frequency modulated continuous waveform (FMCW) radar with synchronized RIS beam sweeping in mmWave has not yet been demonstrated, and here we present an experimental validation of an RIS-enabled NLOS target detection. The RIS-assisted testbed, a bird's eye view illustration of the room and example results are presented in Fig. 1 from left to right, respectively, and are further discussed in the following sections.

2 Experimental Setup and Results

The experimental setup consists of a single universal software radio peripheral (USRP) X410, where two BBox Lite 5G (TMYTEK) frontends are connected to the same device channel, sharing the local oscillator, representing a monostatic radar configuration. The frontends are approximately $4\,\lambda$ apart, and they are configured to transmit and receive simultaneously. An XRifle Dynamic RIS with a 3 dB beamwidth of 3° is placed in front, and its incidence angle is pointing at the transmitting frontend. An obstacle, e.g. a whiteboard, is placed in the room to create an NLOS region for part of the room. From the radar's perspective (see Fig. 2), the target is not directly visible. From the RIS side, synchronized beam sweeping is performed towards the NLOS region.

An FMCW waveform consisting of $10\,\mu$s chirps, spanning a bandwidth of 250 MHz is continuously transmitted in the 28 GHz band. The RIS performs an angular sweep in 1° steps, with each configuration applied for 50 ms, of which only 30 ms are retained for post-processing, while 20 ms are used as a guard time to account for command transmission to the controller and processing on the RIS side. The received IQ samples are aligned with the corresponding RIS configuration and processed to obtain one range profile per RIS configuration, resulting in a range-RIS-angle map.

An empty-room calibration measurement, in which the dominant bins are captured from the RIS sweep, is compared with a second measurement in which the target (a metallic object, refer to Fig. 1) in the NLOS region is present. The RIS beam is commanded in (θ, ϕ) coordinates, where θ is the angle from broadside and ϕ the azimuthal orientation of the steering plane. We fix ϕ and sweep $\theta \in [24°, 57°]$ in 1° steps. The radar, RIS, and target are mounted at the same height, so the sweep remains in the horizontal plane.

After extracting the observed power delay profile (PDP) for each RIS configuration, effectively obtaining the range-RIS-angle map, we subtract the two maps to obtain a "Δ PDP" for each configuration. Subtracting two empty-room captures instead yields no positive Δ PDP value above 0.5 dB, which bounds the detection floor. Some low-power paths (possibly high-order reflections) exhibit negative differences due to shadowing introduced by the target. For target detection, however, the positive side of the Δ PDP is relevant.

One example result is shown in the last plot in Fig. 1, where a 6.5 dB angle-selective enhancement appears at $\theta = 48°$. From in-room geometry calculations, this corresponds to the beam hitting the target. The peak lies at 7.2 m, within the 2.4 m path-length resolution ($2c/B$, Hann window) of the radar-RIS-target-RIS-radar real distance, which is roughly 6.5 m. We can conclude that from the Δ PDP, room geometry and known radar and RIS positions, we can not only detect the presence of a target, but also estimate its position.

Future work will investigate detection without the necessity of calibration, for example via a carefully-designed RIS codebook. Moreover, the evaluation will be extended to moving targets and multiple-target scenarios.

3 Demo Presentation

Due to the size, alignment sensitivity and the necessity for controlled conditions of the complete RIS-assisted radar testbed, the physical equipment will remain in our laboratory. The onsite demonstration will connect to the laboratory through a live video feed showing the NLOS layout representative of the setup presented in this paper, including the radar, RIS, blocking object, and the target. At the conference, previously recorded and newly acquired raw calibration and target measurements will be processed live to construct range–RIS-angle maps and compute the Δ PDP. Attendees will observe how the target-related peak emerges at the predicted RIS steering angle and how the target range and position are estimated from the known room geometry. The authors will operate and explain the demonstration onsite.

Acknowledgments

This work was supported by the Federal Ministry of Research, Technology, and Space (BMFTR, Germany) within the project xG-RIC under grant 16KIS2429K.

References

[1] Stefano Buzzi, Emanuele Grossi, Marco Lops, and Luca Venturino. 2022. Foundations of MIMO Radar Detection Aided by Reconfigurable Intelligent Surfaces. *IEEE Transactions on Signal Processing* 70 (2022), 1749–1763. doi:10.1109/TSP.2022.3157975

[2] Laura Dodds, Hailan Shanbhag, Junfeng Guan, Saurabh Gupta, and Haitham Hassanieh. 2024. Around the Corner mmWave Imaging in Practical Environments. In *30th ACM International Conference on Mobile Computing and Networking (MobiCom 2024)*. ACM, Washington, D.C., 953–967. doi:10.1145/3636534.3690671

[3] Qinpei Luo, Jiahao Gao, and Boya Di. 2024. Horus: Enhancing Safe Corners via Integrated Sensing and Communication Enabled by Reconfigurable Intelligent Surface. In *30th ACM International Conference on Mobile Computing and Networking (MobiCom 2024)*. ACM, Washington, D.C., 2187–2190. doi:10.1145/3636534.3698224

[4] Aadesh Madnaik and Karthikeyan Sundaresan. 2025. Practical Design and Orchestration of Frequency-Shifting RIS for NLoS mmWave Sensing. In *26th ACM International Symposium on Theory, Algorithmic Foundations, and Protocol Design for Mobile Networks and Mobile Computing (MobiHoc 2025)*. ACM, Houston, TX, 91–100. doi:10.1145/3704413.3764440

[5] Timothy Woodford, Kun Qian, and Xinyu Zhang. 2023. Metasight: High-Resolution NLoS Radar with Efficient Metasurface Encoding. In *21st ACM Conference on Embedded Networked Sensor Systems (SenSys 2023)*. ACM, Istanbul, Turkey, 308–321. doi:10.1145/3625687.3625803

[6] Kainat Yasmeen, Debidas Kundu, and Shobha Sundar Ram. 2024. Around-the-corner Radar Sensing Using Reconfigurable Intelligent Surface. In *IEEE Microwaves, Antennas, and Propagation Conference (MAPCON 2024)*. IEEE, Hyderabad, India, 1–4. doi:10.1109/MAPCON61407.2024.10923061

[7] Kaichen Zhou, Laura Dodds, Sayed Saad Afzal, and Fadel Adib. 2026. *RISE: Single Static Radar-based Indoor Scene Understanding*. cs.CV 2511.14019. arXiv. doi:10.48550/arXiv.2511.14019